Author Manuscript

Author Manuscript

Author Manuscript

Author Manuscript

HHS Public Access

Author manuscript

J Nat Prod. Author manuscript; available in PMC 2018 January 27.

Published in final edited form as:

J Nat Prod. 2017 January 27; 80(1): 96–107. doi:10.1021/acs.jnatprod.6b00744.

Nanomolar Antimalarial Agents against Chloroquine-Resistant *Plasmodium falciparum* from Medicinal Plants and Their Structure-Activity Relationships

Bin Zhou[†,⊥], **Yan Wu**[†,⊥], **Seema Dalal**[‡], **Emilio F. Merino**[‡], **Qun-Fang Liu**[†,⊥], **Cheng-Hui Xu**[†,⊥], **Tao Yuan**[†,⊥], **Jian Ding**[†,⊥], **David G. I. Kingston**[§], **Maria B. Cassera**[‡], and **Jian-Min Yue**[*,†,⊥]

[†]State Key Laboratory of Drug Research, Shanghai Institute of Materia Medica, Chinese Academy of Sciences, 555 Zuchongzhi Road, Shanghai 201203; University of Chinese Academy of Sciences, No.19A Yuquan Road, Beijing 100049, People's Republic of China

[‡]Department of Biochemistry and the Virginia Tech Center for Drug Discovery, MC 0308, Virginia Tech, Blacksburg, Virginia 24061, United States

[§]Department of Chemistry and the Virginia Tech Center for Drug Discovery, MC 0212, Virginia Tech, Blacksburg, VA 24061, United States

[⊥]University of Chinese Academy of Sciences, No. 19A Yuquan Road, Beijing 100049, People's Republic of China

Abstract

Inspired by the discovery of the antimalarial drug artemisinin from a traditional Chinese medicine (TCM), a natural product library of 44 lindenane-type sesquiterpenoids was assessed for activities against the Dd2 chloroquine-resistant strain of the malaria parasite *Plasmodium falciparum*. These compounds were mainly isolated from plants of the *Chloranthus* genus, many species of which are named "Sikuaiwa" in TCM and have long been used to treat malaria. The compounds consisted of 41 sesquiterpenoid dimers and three monomers, including the twelve new dimers **1**–**12** isolated from *C. fortunei*. The results showed that 16 dimers exhibited potent antiplasmodial activities (<100 nM); in particular, compounds **1**, **14** and **19** exhibited low nanomolar activities with IC_{50} values ranging from 1 to 7 nM, which is comparable to the potency of artemisinin, and selectivity index values toward mammalian cells greater than 500. A comprehensive structure-activity relationship (SAR) study clearly indicated that three functional groups are essential and two motifs can be modified.

Graphical Abstract

[*]Corresponding Authors: Tel: +86-21-50806718. Fax: +86-21-50806718. jmyue@simm.ac.cn (J.-M. Yue).

The authors declare no competing financial interest.

ASSOCIATED CONTENT

Supporting Information. IR, ESIMS, HRESIMS, 1D and 2D NMR spectra of compounds **1**–**12**, and the purities of compounds **1**–**44** are provided. This material is available free of charge via the Internet at http://pubs.acs.org.

Author Manuscript Author Manuscript Author Manuscript Author Manuscript

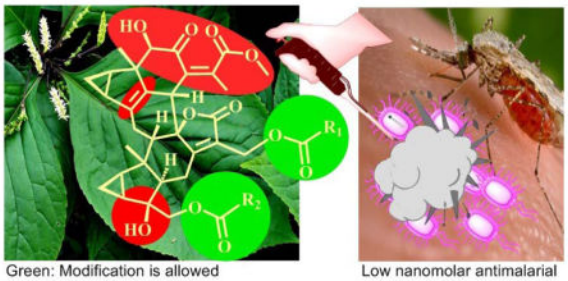

Keywords

Antimalarial activity; Structure-activity relationship; Natural products; Lindenane-type sesquiterpenoids

Malaria is a global parasitic infectious disease caused by *Plasmodium* parasites, which are transmitted by the bite of female anopheles mosquitoes. The disease is widespread in tropical and subtropical regions, with the majority of deaths occurring in Africa and caused by *P. falciparum*, resulting in losses of US $12 billion a year.[1] Approximately 3.2 billion people remain at risk of contracting malaria, leading to an estimated 214 million malaria cases, and 438,000 deaths in 2014 alone.[2] Drug resistance also poses a growing problem for malaria treatment, including the gold standard artemisinin combination therapies.[3] Therefore, the development of new antimalarial agents to expand the repertoire of drugs suitable for use in combination therapies remains a priority to retain effective malaria control and elimination.

The Chloranthaceae family has three genera with a total of 16 species, including *Chloranthus* (thirteen sp.), *Sarcandra* (two sp.), and *Hedyosmum* (one sp.), which are mainly distributed in the southern area of China.[4] Our ongoing studies on plants of the former two genera in the Chloranthaceae family have led to the isolation of a large number of sesquiterpenoids and sesquiterpenoid dimers with diverse bioactivities.[5]

Natural products have played a very important role in antimalarial drug development, and have led to the well-known antimalarial drugs quinine and artemisinin.[6] The potent antimalarial artemisinin was developed from a traditional Chinese medicine, the aerial parts of *Artemisia annua* dubbed “Qinghao”, which was used to treat malaria as early as 340 CE, as documented in the ancient Chinese pharmacopeia “*Principal Prescription Emergency*” in China’s Eastern Jin Dynasty[7] Interestingly, many *Chloranthus* species, called “Sikuaiwa” in TCM, were also used for the same purpose.[8] A small library of structurally related compounds isolated from five *Chloranthus* species and one *Sarcandra* specie was thus subjected to antiplasmodial bioassay against the chloroquine-resistant Dd2 strain of *P. falciparum*. These compounds included three lindenane-type sesquiterpenoid monomers and 41 dimers (Figures 1–3). Compounds **1**–**12** are new dimeric sesquiterpenoids isolated from the twigs of *C. fortunei* and reported in this study. The antiplasmodial screening revealed that several of the sesquiterpenoid dimers exhibited very potent antiplasmodial activities, and three compounds had potent activities similar to that of artemisinin. These results open

Author Manuscript Author Manuscript Author Manuscript Author Manuscript

the way to further studies on this new class of promising antiplasmodial compounds that may act through a new mechanism of action because of their unique structural architectures. We herein present the isolation and structure elucidation of the new compounds, as well as the antiplasmodial activities and structure-activity relationships of all 44 compounds.

RESULTS AND DISCUSSION

Compound **1** had a molecular formula of $C_{41}H_{46}O_{14}$ as determined by the sodiated (+)-HRESIMS ion at *m/z* 785.2781 $[M + Na]^+$ (calcd 785.2780) and ^{13}C NMR data. Analysis of the NMR data (Tables 1 and 4) suggested that **1** is a lindenane-type sesquiterpenoid dimer with the distinct features of two 1,2-substituted cyclopropane rings, one α,β-unsaturated-γ-lactone, and a persubstituted double bond. Comprehensive analysis of the 1D and 2D NMR data further revealed that its structure is similar to that of chlorajaponol G[9] except for the presence of a γ-formylsenecioate motif instead of the angeloate moiety of the latter. This conclusion was verified by HMBC correlations of H-4″ (δ_H 9.67)/C-2″ and C-5″ within the motif that was attached to C-15′ by the key HMBC correlation from H_2-15′ to C-1″ (δ_C 165.5) (Figure 4A). Additionally, a methyl succinoate group was attached to C-13′ as indicated by the key HMBC correlation of H_2-13′/C-9″ (δ_C 172.1). The relative configuration of **1** was assigned primarily by its ROESY data (Figure 4B), in which the correlations of H-1/H-2α, H-1/H-3, H-1/H-9, H-1′/H-2′α, H-2′α/H-3′, H-3′/H-15′, and H-5′/H-15′ indicated that they are spatially close and assigned arbitrarily as α-oriented. Accordingly, the ROESY correlations of H-2β/H_3-14, H_3-14/H-6, H-2′β/H_3-14′, and H_3-14′/H-9′ revealed that they were β-oriented. The $\Delta^{2''}$ double bond was assigned *E* by the ROESY correlation of H_2-4″/H-2″. Thus, the structure of fortunilide A (**1**) was depicted as shown.

The molecular formula of compound **2** was established as $C_{41}H_{48}O_{14}$, by the sodium adduct (+)-HRESIMS ion at *m/z* 787.2964 $[M + Na]^+$ (calcd 787.2936) and the ^{13}C NMR data. The NMR data (Tables 1 and 4) of **2** showed many similarities to those of shizukaol F,[10] suggesting that they are structural analogues. Comprehensive analysis of the spectroscopic data of **2** revealed that it shared the same dimeric sesquiterpenoid core with shizukaol F and the structural differences were the substituent groups at C-13′ and C-15′. Compound **2** was assigned as a methanolysis product of shizukaol F with the cleavage between C-13′ and C-9″ in the 18-membered macrocyclic trilactone of the latter. This conclusion was confirmed by the HMBC correlations (Figure S13, Supporting Information) from H-4″ (δ_H 4.62) to C-2″ (δ_C 114.8) and C-6″ (δ_C 171.8), from both H-7″ (δ_H 2.67) and H-8″ (δ_H 2.73) to C-6″ and C-9″ (δ_C 173.0), and from OC$\underline{H_3}$ (δ_H 3.67) to C-9″. The relative configuration of **2** was established by ROESY data (Figure S14, Supporting Information), in particular, the $\Delta^{2''}$ double bond was assigned as *E*-geometry by the key ROESY interaction between H-4″ and H-2″. Hence, the structure of **2**, fortunilide B, was unequivocally characterized.

Compound **3** had the molecular formula $C_{36}H_{42}O_{10}$ based on its ^{13}C NMR data and sodium adduct (+)-HRESIMS ion at *m/z* 657.2672 $[M + Na]^+$ (calcd 657.2670). Analysis of its NMR data (Tables 1 and 4) revealed that its structure is closely related to that of shizukaol K[11] with the differences being the substituents at C-13′ and C-15′. The presence of a

Author Manuscript Author Manuscript Author Manuscript Author Manuscript

senecioate moiety was identified by HMBC correlations within this motif, and its attachment to C-15′ was indicated by the key HMBC cross-peak from H_2-15′ (δ_H 4.83 and 4.10) to C-1″ (δ_C 166.8) (Figure S22, Supporting Information). A hydroxy group was located at C-13′ by the chemical shifts of H-13′ (δ_H 4.41 and 4.34, each 1H, d, J = 13.6 Hz) and C-13′ (δ_C 54.9). A ROESY experiment (Figure S23, Supporting Information) showed that the relative configuration of **3** was identical to that of shizukaol K. The structure of compound **3**, fortunilide C, was thus established as shown.

The molecular formula, $C_{41}H_{48}O_{16}$, of compound **4** was determined by its sodium adduct (+)-HRESIMS ion at *m/z* 819.2851 $[M + Na]^+$ (calcd 819.2835). Detailed analysis of its NMR data (Tables 1 and 4) revealed it to be a methanolysis product of spicachlorantin D[12] with the cleavage between C-13′ and C-9″ in the 18-membered macrocyclic trilactone of the latter. This conclusion was confirmed by the HMBC correlations (Figure S31, Supporting Information) from H-4″ (δ_H 4.66) to C-2″ (δ_C 115.2) and C-6″ (δ_C 171.9), from both H-7″ (δ_H 2.67) and H-8′ (δ_H 2.73) to C-6″ and C-9″ (δ_C 173.0), and from $OC\underline{H_3}$ (δ_H 3.69) to C-9″. In addition, a characteristic singlet signal at δ_H 8.64 (OOH) and a quaternary carbon resonance at δ_C 90.8 indicated the presence of a hydroperoxy group at C-4.[12] The relative configuration of **4** was identical to that of spicachlorantin D as indicated by its ROESY data (Figure S32, Supporting Information). The structure of **4**, fortunilide D, was thereby determined as shown.

Compound **5** had the same molecular formula $C_{41}H_{48}O_{16}$ as **4**, as determined by the (+)-HRESIMS ion at *m/z* 819.2842 $[M + Na]^+$ (calcd 819.2835) and ^{13}C NMR data. Analysis of the NMR data (Tables 2 and 4) revealed that **4** and **5** were isomers, with differing substituents at C-13′ and C-15′. A methyl succinoate and a γ-hydroxysenecioate moieties were attached to C-13′ and C-15′ of **5** as shown by the key HMBC correlations of H_2-13′/C-9″ and H_2-15′/C-1″ (Figure S40, Supporting Information), respectively. The $\Delta^{2''}$ double bond was assigned as *E* by the ROESY interaction between H_2-4″ and H-2″ (Figure S41, Supporting Information). Thus, the structure of fortunilide E (**5**) was unequivocally characterized as shown.

Compound **6** had the molecular formula $C_{31}H_{36}O_{10}$, based on its (+)-HRESIMS ion at *m/z* 591.2211 $[M + Na]^+$ (calcd 591.2201) and ^{13}C NMR data. Comparison of its NMR data (Tables 2 and 4) with those of spicachlorantin J[13] revealed that their structures are closely related and both of them possessed a hydroperoxy moiety at C-4. The only variation was the presence of a hydroxymethyl group at C-4′ in **6** instead of the exocyclic $\Delta^{4'(15')}$ double bond in the latter, as supported by the HMBC correlations from H_2-15′ (δ_H 3.57 and 3.35) to C-3′, C-4′, and C-5′ (Figure S49, Supporting Information). The structure of **6**, fortunilide F, was finally confirmed by the HMBC and NOESY spectra (Figure S50, Supporting Information).

Compound **7** had the molecular formula $C_{40}H_{44}O_{13}$ as determined by the mass of the sodiated molecular ion at *m/z* 755.2683 $[M + Na]^+$ (calcd 755.2674) in the (+)-HRESIMS and the ^{13}C NMR data. The NMR data (Tables 2 and 4) of **7** showed strong similarities to those of henriol C[14] except for the changes regarding the location of CH_3-5″, which was attached to C-3″ in the lactone bridge of **7** instead of C-2″ in that of henriol C, as deduced

Author Manuscript Author Manuscript Author Manuscript Author Manuscript

by the key HMBC correlation from H-5″ to C-4″. The chemical shift of H_2-4″ (δ_H 4.71) suggested an *E*-geometry[15] for the $\Delta^{2''}$ double bond in the macrolide motif. The structure of **7**, fortunilide G, was further verified by HMBC and ROESY spectra (Figures S58 and S59, Supporting Information).

Compound **8**, named fortunilide H, was assigned the molecular formula $C_{40}H_{44}O_{14}$ on the basis of its (+)-HRESIMS ion at *m/z* 771.2625 (calcd 771.2623) and its ^{13}C NMR data. Analysis of the NMR data (Tables 2 and 4) showed many similarities with those of chloramultiol F,[16] with a large conjugated system of two additional double bonds and one α,β-unsaturated-γ-lactone. The main differences were the presence of methyl succinoate and γ-hydroxysenecioate residues at C-13′ and C-15′, respectively, instead of the 18-membered macrocyclic trilactone ring of chloramultiol F. The locations of these groups were assigned by the HMBC correlations of H_2-13′/C-9″ and H_2-15′/C-1″ (Figure S67, Supporting Information). In addition, a hydroxy group was placed at C-8 by the chemical shift (δ_C 104.7) instead of the methoxy group in chloramultiol F, which was assigned as α-oriented by the pyridine-induced solvent shifts for H-5′ ($\Delta\delta = -0.63$).[17] The $\Delta^{2''}$ double bond was assigned as *E*-geometry by the key ROESY correlation of H_2-4″/C-2″ (Figure S68, Supporting Information). The structure of **8** was further verified by 2D NMR spectra.

Compound **9** had the molecular formula $C_{40}H_{46}O_{16}$, as determined by its (+)-HRESIMS ion peak at *m/z* 805.2659 $[M + Na]^+$ (calcd 805.2678) and ^{13}C NMR data. The NMR data (Tables 3 and 4) of **9** showed many similarities to those of **8**, suggestive of structural analogues. In particular, an oxygenated quaternary carbon signal (δ_C 89.9, C-4) and a methylene carbon signal (δ_C 36.1, C-15) were observed for **9** in place of the carbon signals of an $\Delta^{4(15)}$ double bond for **8**, indicating the presence of a hydroperoxy moiety at C-4. Two groups of a methyl succinoate and a γ-hydroxysenecioate were assigned to C-13′ and C-15′ respectively by the HMBC correlations of H_2-13′/C-9″ and H_2-15′/C-1″ (Figure S76, Supporting Information). 8-OH was assigned as α-oriented by the pyridine-induced solvent shifts for H-5′ ($\Delta\delta = -0.74$).[17] The structure of fortunilide I (**9**) finally confirmed by HMBC and ROESY data (Figure S77, Supporting Information), was elucidated as shown.

Compound **10**, named fortunilide J, was obtained as a white amorphous powder. A molecular formula of $C_{35}H_{40}O_{11}$ was assigned for **10** with 16 DBEs on the basis of its (−)-HRESIMS ion at *m/z* 635.2475 $[M - H]^-$ (calcd 635.2498) as well as its ^{13}C NMR data. Analysis of the NMR data (Tables 3 and 4) suggested that **10** is a lindenane-type sesquiterpenoid dimer with the distinct features of two 1,2-substituted propane rings, two α,β-unsaturated-γ-lactone groups, a trisubstituted double bond and a γ-hydroxysenecioate residue. Comprehensive investigation of the spectroscopic data including 2D NMR revealed that it is structurally related to henriol B,[14] and the differences were the presence of a $\Delta^{4(15)}$ double bond instead of the Δ^5 double bond of the latter, and the γ-hydroxysenecioate residue in place of the senecioate residue of henriol B. The different position of the double bond was confirmed by the key HMBC correlations (Figure 5A) from H-15 (δ_H 5.82) to C-3 and C-8′ (δ_C 92.0), and from H-6 to C-4 (δ_C 146.1). In addition, the γ-hydroxysenecioate group was attached to C-15′ by the HMBC correlations of H_2-15′/C-1″ (δ_C 168.3). The relative configuration of **10** was verified mainly by its ROESY data (Figure 5B), in which ROESY correlations of H-1/H-2α, H-1/H-3, H-1/H-9, H-1′/H-2′α, H-2′α/H-3′, H-3′/H-15′, and

Author Manuscript Author Manuscript Author Manuscript Author Manuscript

H-5′/H-15′ showed that these protons were co-facial and were assigned arbitrarily as α-oriented. In consequence, the ROESY correlations of H-2β/H_3-14, H_3-14/H-5, H_3-14/H-6, H-2′β/H_3-14′, and H_3-14′/H-9′ indicated that they were β-oriented The $\Delta^{2''}$ double bond was assigned as *E* by the ROESY correlation of H_2-4″/H-2″. The 8-OH was assigned as α by the significant pyridine-induced solvent shift[17] for H-5′ ($\Delta\delta = -0.81$).

Compound **11** was obtained as a colorless gum and was assigned the molecular formula $C_{36}H_{40}O_9$ by the (−)-HRESIMS ion peak at *m/z* 615.2588 $[M - H]^-$ (calcd for 615.2600), requiring 17 double bond equivalents (DBE). The IR spectrum revealed the presence of hydroxy (3455 cm^{-1}), carbonyl (1761 cm^{-1}), and olefinic (1656 cm^{-1}) functionalities. Initial analysis of the NMR data (Tables 3 and 4) of **11** suggested it was a lindenane-type sesquiterpenoid dimer possessing the rare sarcanolide A skeleton.[18] Comprehensive analysis of the 1D and 2D NMR spectra of **11** further revealed that the only structural difference between it and sarcanolide A was the existence of Δ^4 double bond in place of the 4,5-diol of the latter. This was verified by the multiple HMBC correlations (Figure 6) of H-15/C-4 (δ_C 151.3) and C-5 (δ_C 135.4), and H-14/C-5. The unique β-directed 3-methylenedihydrofuran-2(3H)-one motif was deduced by the key HMBC correlations from H-13′ (δ_H 5.52 and 6.20) to C-7′, C-11′ (δ_C 145.9), and C-12′ (δ_C 168.4). The tigloyl unit was assigned to C-15′ by the key HMBC correlation from H-15′ to C-1″ (δ_C 167.9). The relative configuration of **1** was elucidated by its ROESY data (Figure 6), which is similar to that of sarcanolide A, except for that CH_3-13 was assigned as α-configured on the basis of the strong correlation between H_3-13 and H-6′α. The structure of compound **11** (fortunilide K) was hence characterized as shown.

Fortunilide L (**12**) had the molecular formula $C_{41}H_{46}O_{13}$ as determined by its (+)-HRESIMS ion at *m/z* 769.2830 $[M + Na]^+$ (calcd 769.2831), requiring 19 DBEs. Detailed analysis of NMR data (Tables 3 and 4) of **12** showed that it shared a common dimeric sesquiterpenoid core with **11**, and the only structural difference was in the substituent at C-15′. HMBC correlations (Figure 6) within the substituent confirmed it to be an (*E*)-4-((4-methoxy-4-oxobutanoyl)oxy)-2-methylbut-2-enoyloxy group, and it was assigned to C-15′ by the HMBC correlations from H-15′ to C-1″. The *E*-configuration of the $\Delta^{2''}$ double bond was assigned based on the ROESY cross-peak between H_2-4″ and H-2″ (Figure S105, Supporting Information). The structure of **12** was thus established as depicted.

The 15 known lindenane-type sesquiterpenoid dimers, sarglabolide I,[19] sarglabolide J,[19] shizukaol F,[10] shizukaol K,[11] shizukaol I,[10] shizukaol C,[20] shizukaol M,[11] chlorajaponilide C,[21] chlorahololides D,[5j] spicachlorantin D,[12] chloramultilide C,[22] shizukanolide F,[23] chloranthalactone C,[24] and isoshizukanolide,[25] and sarcandrolide J[5a] were also isolated and identified by spectroscopic data and analogy with the reported data in literature.

Antiplasmodial Activity and Structure-Activity Relationships

A total of 44 structurally related compounds obtained from our previous studies were assessed for potential antiplasmodial activity. Twelve new compounds fortunilides A-L (**1**–**12**), as well as 10 known analogues sarglabolide I (**13**), sarglabolide J (**14**), shizukaol K (**15**), shizukaol I (**16**), shizukaol C (**17**), schizukaol M (**18**), chlorahololide D (**20**), shizukanolide

Author Manuscript Author Manuscript Author Manuscript Author Manuscript

F (**42**), chloranthalactone C (**43**), and isoshizukanolide (**44**) were isolated currently from *C. fortunei*. Chloraholide A (**33**),[15b] chloraholide C (**34**),[17b] and chloraholide E (**38**)[17b] were obtained from *C. holosteigius*. Chloramultilide A (**35**),[26] chloramultilide D (**37**),[22] chloramultilide C (**39**),[22] and chloramultilide B (**41**)[22] came from *C. multisachys*. Chlorajaponilide C (**19**),[21] shizukaol N (**21**),[11] shizukaol E (**25**),[10] shizukaol D (**26**),[20] shizukaol F (**28**),[10] shizukaol G (**29**),[10] shizukaol B (**30**),[20] spicachlorantin D (**31**),[27] shizukaol A (**32**),[28] and spicachlorantin B (**40**)[29] were isolated from the plants *C. serratus* and *C. spicatus*. Sarcandrolide B (**22**),[5b] sarcandrolide A (**23**),[5b] sarcandrolide J (**24**),[5a] sarcandrolide E (**27**),[5b] and sarcandrolide D (**36**)[5b] were isolated from *S. glabra*.

The antiplasmodial activities of all the compounds were tested using a SYBR-Green assay against *P. falciparum* strain Dd2 (chloroquine-resistant) with artemisinin as the positive control as described previously.[30,31] Sixteen compounds exhibited IC_{50} values below 100 nM, eight compounds showed mid to high nanomolar IC_{50} values (100–860 nM), eight compounds were in the micromolar range, and the others were inactive at 25 μM, which was the highest concentration tested (Table 5). Fifteen of the compounds that exhibited IC_{50} values below 100 nM were tested for mammalian cytotoxicity toward normal embryonic lung tissue (WI-38 cell line). Nine of the 15 compounds presented a selectivity index (SI) value of ≥100 (Table 6). Compounds **1**, **14**, and **19** had IC_{50} values of 5.2 ± 0.6, and 7.2 ± 1.3, and 1.1 ± 0.2 nM, respectively, and thus have similar potencies to the positive control artemisinin (IC_{50} = 4.0 ± 4.2 nM). Moreover, these compounds showed a SI value of 1,700, 561 and 4,900 respectively (Table 6) supporting their selective activity against the malaria parasite.

To assess the structure-activity relationships of this new class of antiplasmodial compounds, we first compared the structures of the most active compounds, **1**, **2**, **7**, **14**, **17**–**21**, and **28**–**30** with those inactive and/or less potent compounds, **10**, **13**, **24**, **25**, **27**, **32**–**44** (Figures 1–3) in Table 5. All the active compounds against *P. falciparum* are lindenane-type sesquiterpenoid dimers, and the three lindenane-type sesquiterpenoid monomers tested (**42**–**44**) were inactive. The most active dimers, e.g. compounds **1**, **2**, **14**, **17**, **19**, **20**, and **28**–**30**, featured the common motifs of a conjugated system of methyl (*Z*)-5-hydroxy-4-oxopent-2-enoate, a Δ^4 double bond, and a hydroxy group at C-4′ as marked in red. All the compounds without methyl (*Z*)-5-hydroxy-4-oxopent-2-enoate and/or Δ^4 double bond motifs showed marginal activities or were inactive. Compounds **20** and **27** showed very similar structures except for the facts that **20** (13 ± 3 nM) had a Δ^4 double bond, while **27** (> 25 μM) possessed a 4-OH and Δ^5 double bond, suggesting that a Δ^4 double bond is necessary for the activity, and this was supported by the very similar observations between compounds **30** (27 ± 3 nM) and **35** (>25 μM). Moreover, a similar observation between compounds **19** and **5** was observed where the absence of the Δ^4 double bond in compound **5** reduced the antiplasmodial activity about 4-fold; however, the toxicity toward mammalian cells was also tremendously reduced since no toxicity was observed for compound **5** at 100 μM (Table 6). Interestingly, the absence of the Δ^4 double bond in compound **4** reduced the antiplasmodial activity by less than 1-fold as compared with the structurally similar counterpart compound **2**; however, the toxicity toward mammalian cells was also increased by 6-fold (Table 6). The absence of the 4′-OH renders the compounds less active as compared with structurally

Author Manuscript Author Manuscript Author Manuscript Author Manuscript

similar counterparts, e.g. the compound pairs **21** (100 ± 10 nM)/**26** (without 4′-OH, 580 ± 90 nM), and **13** (4.6 ± 0.2 μM)/**24** (without 4′-OH, 11.4 ± 1.6 μM), and this was consistent with the fact that compounds **25** and **32** without 4′-OH groups also showed *P. falciparum* growth inhibition in the micromolar range. The rare dimeric compounds **11** and **12** without the (*Z*)-configured $\Delta^{7(11)}$ double bond showed attenuated antiplasmodial activities with IC_{50} values of 4.7 ± 0.5 μM and 99 ± 18 nM, respectively, as compared with their structurally similar analogues **2**, **17**, and **20**. In addition, when the methyl (*Z*)-5-hydroxy-4-oxopent-2-enoate motif of compound **28** (11 ± 1 nM) changed to the *E*-geometry of **7** (48 ± 12 nM), the antiplasmodial activity was reduced about 4-fold, suggesting that the motif with a *Z*-geometry seemed more favorable for the antiplasmodial activity. However, both compounds showed SI values below 30 where the *E*-geometry also decreased the mammalian cytotoxicity by 5-fold (Table 6). Furthermore, compound **8** (198 ± 22 nM) had a very similar structure with that of the most potent antiplasmodial compound **19** (1.1 ± 0.2 nM) except for the absence of the Δ^4 double bond (replaced by $\Delta^{4(15)}$ and Δ^5 double bonds) and the methyl (*Z*)-5-hydroxy-4-oxopent-2-enoate motif (ring closed to a five-membered α,β-unsaturated semiketal lactone), suggesting that these two groups are very important for the antiplasmodial activity observed with compound **19**.

Interestingly, the presence of two ester chains R^1 and R^2 at C-13′ and C-15′, respectively, dramatically improves the antiplasmodial activities as observed for the low nanomolar antiplasmodial compounds **1**, **14**, and **19**. When the R^1 ester group was absent, for example compounds **2**, **17**, **18**, and **21**, the antiplasmodial potencies were reduced considerably. In addition, when the two ester chains formed an 18-membered macrocyclic trilactone ring, e.g. compounds **7**, **28–30**, the antiplasmodial potencies were slightly reduced as compared with the ring-opened analogues. For the compounds possessing the 18-membered macrocyclic trilactone rings, the antiplasmodial activities of compounds with an *E*-acyloxy-3-methylbut-2-enoate (**28** and **41**) were better than those with an *E*-acyloxy-2-methylbut-2-enoate (**30** and **39**); however, those with those with an *E*-acyloxy-2-methylbut-2-enoate showed lower mammalian cytotoxicity and better SI values. The presence of a 7′′α-OH at the 18-membered macrocyclic trilactone ring (**29**, 13 ± 1 nM) also increased the potency as compared with compound **30** (27 ± 3 nM), however, also increased mammalian cytotoxicity by ~10-fold (Table 6). It is evident that chain lengths, geometry of the double bonds, and oxidation patterns of the R^1 and R^2 motifs influence the *P. falciparum* growth inhibition activities significantly, indicating that the R^1 and R^2 motifs can be modified to improve the antiplasmodial activities of this compound class.

Compounds **4**, **5**, **9**, and **31** with a hydroperoxy group at C-4 (4-OOH) and Δ^5 double bond showed remarkable antiplasmodial activities with IC_{50} values ranging from the low nanomolar to the low micromolar range (Table 5). These potencies are much stronger than those predicted by the previous SAR results, with inactive analogues **27**, **33–35** bearing a 4-OH and Δ^5 double bond (Figures 1 and 3), suggesting that the 4-OOH is the crucial moiety for this antiplasmodial compound subclass that likely operates by a different mechanism and/or has a different SAR than the other active dimers. On the other hand, the absence of the 4′-OH group and the two acyl groups at C-13′ and C-15′ reduced antiplasmodial potency dramatically. Thus compound **6** (5.3 ± 2 μM) is much less active than compound **4**

Author Manuscript Author Manuscript Author Manuscript Author Manuscript

and **5**, indicating that the 4′-OH and the two ester chains R^1 and R^2 at C-13′ and C-15′ are also important motifs for the antiplasmodial activities for this compound subclass.

Taken together, the above analysis has outlined a clear SAR for the tested compounds as follows (Figure 7). (1) All the active compounds are the Diels-Alder adducts of lindenane-type sesquiterpenoid dimers, while the monomers were inactive. (2) The most potent dimers feature common motifs of a Δ^4 double bond, a 4′-OH, and a conjugated system of methyl (*Z*)-5-hydroxy-4-oxopent-2-enoate. (3) The presence of two ester chains R^1 and R^2 at C-13′ and C-15′, respectively, dramatically affects the antiplasmodial activities, suggesting that these groups can be modified to improve the antiplasmodial potency of this class of compounds. (4) For the 4-OOH compound subclass, the 4-OOH moiety is the crucial motif for the antiplasmodial activity, which likely operates by a different mechanism and/or has a different SAR than the other active dimers.

In conclusion, a new class of potent antiplasmodial agents against the chloroquine-resistant strain of *P. falciparum* with low mammalian cytotoxicity was discovered from the plants of *Chloranthus* genus known as “sikuaiwa”, which have long been used in traditional Chinese medicine to treat malaria. Among the active compounds, three of them presented low nanomolar IC_{50} values antiplasmodial similar to artemisinin and a selectivity index value of ≥500. A SAR study of this new class has also been performed and clearly indicated that two motifs in this class can been modified to enhance the antiplasmodial potency. Therefore, lindenane sesquiterpnoid dimers are new class of promising antiplasmodial agents, and likely act through a new mode-of-action because of their unique scaffold that is different from all currently known antiplasmodial agents. Further investigation of this new antiplasmodial class is thus warranted and is currently underway.

EXPERIMENTAL SECTION

General Experimental Procedures—Optical rotations were recorded on an Autopol VI polarimeter. The UV data were obtained by using a Shimadzu UV-2550 spectrophotometer. The IR spectra were acquired on a Thermo IS5 spectrometer with KBr disks. The NMR spectra were run on a Bruker AM-500 spectrometer with TMS as internal standard. The ESIMS and HRESIMS were obtained on a Brucker Daltonics Esquire 3000 plus and a Waters-Micromass Q-TQF Ultima Global mass spectrometer, respectively. Semipreparative HPLC was performed on a Waters 1525 binary pump system with a Waters 2489 detector (210 nm) using a YMC-Pack ODS-A (250×10 mm, *S*-5 μm). Silica gel (200–300 mesh, Qingdao Haiyang Chemical Co., Ltd), C_{18} reversed-phase (RP-18) silica gel (20–45 μM, Fuji Silysia Chemical LTD), CHP20P MCI gel (75–150 μm, Mitsubishi Chemical Corporation), D101-macroporous absorption resin (Shanghai Hualing Resin Co., Ltd), and Sephadex LH-20 gel (Amersham Biosciences) were used for column chromatography (CC). Precoated silica gel GF_{254} plates (Qingdao Haiyang Chemical Co., Ltd.) were used for TLC monitors. All the solvents used for CC were of analytical grade (Shanghai Chemical Reagents Co., Ltd.), and the solvents used for HPLC were of HPLC grade (J & K Scientific Ltd.).

Author Manuscript Author Manuscript Author Manuscript Author Manuscript

Plant Material—Twigs of *C. fortunei* were collected in June of 2013 in Guilin city, Guangxi Province, China, and were authenticated by Professor Shao-Qing Tang of Guangxi Normal University. A voucher specimen has been deposited in Shanghai Institute of Materia Medica, Chinese Academy of Sciences (accession no: CHF-2011-1Y).

Extraction and Isolation—Dried powder of *C. fortunei* (5 kg) was extracted with 95% EtOH at room temperature to give a crude extract (520 g), which was then partitioned between EtOAc and H_2O. The EtOAc soluble fraction (230 g) was subjected to CC (D101-macroporous absorption resin) eluted with 30%, 50%, 80% and 95% MeOH in H_2O to give four fractions 1–4, respectively. Fraction 2 (120 g) was separated by an MCI gel column (MeOH/H_2O, 4:6 to 9:1) to afford three fractions A–C, and fraction 3 (100 g) was treated similarly to afford two fractions D and E. Fraction A (15g) was chromatographed over a silica gel column and eluted with petroleum ether-acetone (from 50:1 to 1:5) in gradient to afford seven subfractions A1–A7. Fraction A2 (600 mg) was purified by semipreparative HPLC (50% CH_3CN in H_2O, 3 mL/min) to yield shizukanolide F (4.7 mg), chloranthalactone C (5.7 mg), and isoshizukanolide (3.7 mg). Fraction A6 (1.3 g) was chromatographed over a column of Sephadex LH-20 to yield three major parts, and each of them was purified by semipreparative HPLC (65% CH_3OH in H_2O, 3 mL/min) to give shizukaol F (10 mg), shizukaol K (8.3 mg), chlorajaponilide C (11 mg), and chloraholide D (6.5 mg). Fraction A7 (6.1g) was further separated on a column of reversed phase C_{18} silica gel (30–80% MeOH in H_2O) to yield three major components (A7a–A7c). Component A7a (3.5 g) was fractioned on a silica gel column ($CHCl_3$-MeOH, 500:1 to 50:1) to give four major parts A7a1–A7a4. Fraction A7a1 (80 mg) was purified by semipreparative HPLC (55% CH_3CN in H_2O, 3 mL/min) to yield compounds **11** (9.5 mg). In the same ways, fraction A7a2 (400 mg) gave **1** (2.2 mg) and shizukaol I (3.7 mg); fraction A7a3 (1.5 g) yielded compounds **2** (44 mg), **4** (4.7 mg), **5** (43 mg), **7** (22 mg), and spicachlorantin D (3 mg). Fraction A7a4 (900 mg) was chromatographed over a column of Sephadex LH-20 to yield three major parts, and each of them was purified by semipreparative HPLC (40% CH_3CN in H_2O, 3 mL/min) to give **8** (3.0 mg), **10** (8.3 mg), sarglabolide I (5.8 mg), chloramultilide C (3.3 mg), and sarcandrolide J (6.8 mg). By the similar separating procedures used in fraction A, fraction D (52 g) was successively subjected to silica gel column (petroleum ether-acetone: 10:1 to 1:5), Sephadex LH-20 (eluted with EtOH), reversed phase C_{18} silica gel column (MeOH, 30–80%), silica gel column ($CHCl_3$-MeOH, 100:1 to 10:1), and finally purified by semipreparative HPLC to yield **3** (49 mg), **6** (23 mg), **9** (4.0 mg), **12** (28 mg), shizukaol C (23 mg), shizukaol M (13 mg), and sarglabolide J (23 mg).

Fortunilide A (**1**): white, amorphous powder; $[\alpha]^{24}_{D}$ −14.8 (*c* 0.2, MeOH); UV(MeOH) λ_{max} (log ε) 222 (4.40) nm; IR (KBr) ν_{max} 3446, 2926, 1733, 1632, 1438, 1384, 1223,1159, 1037, 991 $cm^{-1;}$ ^1H NMR data ($CDCl_3$), see Table 1 and ^{13}C NMR ($CDCl_3$), see Table 4; (+)-ESIMS *m/z* 785.3 $[M + Na]^+$; (−)-ESIMS *m/z* 761.9 $[M - H]^-$; (+)-HRESIMS *m/z* 785.2781 [M + Na+$^+$ (calcd for $C_{41}H_{46}O_{14}Na$, 785.2780).

Fortunilide B (**2**): white, amorphous powder; $[\alpha]^{24}_{D}$ −115.1 (*c* 1.0, MeOH); UV(MeOH) λ_{max} (log ε) 219 (4.49) nm; IR (KBr) ν_{max} 3458, 2952, 1736, 1604, 1438, 1376, 1225,1157,

Author Manuscript Author Manuscript Author Manuscript Author Manuscript

1086, 991 $cm^{-1;}$ ^{1}H NMR data ($CDCl_3$), see Table 1 and ^{13}C NMR ($CDCl_3$), see Table 4; (+)-ESIMS *m/z* 787.2 $[M + Na]^+$; (−)-ESIMS *m/z* 763.2 $[M - H]^-$; (+)-HRESIMS *m/z* 787.2964 $[M + Na]^+$ (calcd for $C_{41}H_{48}O_{14}Na$, 787.2936).

Fortunilide C (**3**): white, amorphous powder; $[\alpha]^{24}_D$ −152.6 (*c* 1.0, MeOH); UV(MeOH) λ_{max} (log ε) 219 (4.50) nm; IR (KBr) ν_{max} 3465, 2949, 1739, 1601, 1437, 1383, 1228, 1144, 991 $cm^{-1;}$ ^{1}H NMR data ($CDCl_3$), see Table 1 and ^{13}C NMR ($CDCl_3$), see Table 4; (+)-ESIMS *m/z* 657.2 $[M + Na]^+$; (−)-ESIMS *m/z* 633.3 $[M - H]^-$; (+)-HRESIMS *m/z* 657.2672 $[M + Na]^+$ (calcd for $C_{36}H_{42}O_{10}Na$, 657.2670).

Fortunilide D (**4**): white, amorphous powder; $[\alpha]^{24}_D$ −79.5 (*c* 0.5, MeOH); UV(MeOH) λ_{max} (log ε) 219 (4.47) nm; IR (KBr) ν_{max} 3454, 2952, 1735, 1438, 1277, 1223, 1153, 976 $cm^{-1;}$ ^{1}H NMR data ($CDCl_3$), see Table 1 and ^{13}C NMR ($CDCl_3$), see Table 4; (+)-ESIMS *m/z* 819.2 $[M + Na]^+$; (−)-ESIMS *m/z* 795.3 $[M - H]^-$; (+)-HRESIMS *m/z* 819.2851 $[M + Na]^+$ (calcd for $C_{41}H_{48}O_{16}Na$, 819.2835).

Fortunilide E (**5**): white, amorphous powder; $[\alpha]^{24}_D$ −94.2 (*c* 0.9, MeOH); UV(MeOH) λ_{max} (log ε) 219 (4.44) nm; IR (KBr) ν_{max} 3442, 2955, 1736, 1439, 1280, 1216, 1151, 976 $cm^{-1;}$ ^{1}H NMR data ($CDCl_3$), see Table 2 and ^{13}C NMR ($CDCl_3$), see Table 4; (+)-ESIMS *m/z* 778.9 $[M - H_2O + H]^+$; (+)-HRESIMS *m/z* 819.2840 $[M + Na]^+$ (calcd for $C_{41}H_{48}O_{16}Na$, 819.2835).

Fortunilide F (**6**): white, amorphous powder $[\alpha]^{24}_D$ −130.2 (*c* 0.8, MeOH); UV(MeOH) λ_{max} (log ε) 227 (4.24) nm; IR (KBr) ν_{max} 3436, 2925, 2878, 1735, 1677, 1434, 1383, 1109, 971 $cm^{-1;}$ ^{1}H NMR data (CD_3OD), see Table 2 and ^{13}C NMR (CD_3OD), see Table 4; (+)-ESIMS *m/z* 569.3 $[M + H]^+$, 1159.6 $[2\ M + Na]^+$; (+)-HRESIMS *m/z* 591.2211 $[M + Na]^+$ (calcd for $C_{31}H_{36}O_{10}Na$, 591.2201).

Fortunilide G (**7**): white, amorphous powder; $[\alpha]^{24}_D$ −49.8 (*c* 0.7, MeOH); UV (MeOH) λ_{max} (log ε) 213 (4.37) nm; IR (KBr) ν_{max} 3371, 2941, 2855, 1751, 1658, 1438, 1223, 1158, 998, 871 $cm^{-1;}$ ^{1}H NMR data ($CDCl_3$), see Table 2 and ^{13}C NMR ($CDCl_3$), see Table 4; (+)-ESIMS *m/z* 755.3 $[M + Na]^+$; (−)-ESIMS *m/z* 731.7 $[M - H]^-$; (+)-HRESIMS *m/z* 755.2683 $[M + Na]^+$ (calcd for $C_{40}H_{44}O_{13}Na$, 755.2674).

Fortunilide H (**8**): white, amorphous powder; $[\alpha]^{24}_D$ −45.1 (*c* 0.8, MeOH); UV(MeOH) λ_{max} (log ε) 215 (4.46) nm; IR (KBr) ν_{max} 3432, 2923, 1761, 1655, 1387, 1223, 1153, 1075 $cm^{-1;}$ ^{1}H NMR data ($CDCl_3$), see Table 2 and ^{13}C NMR ($CDCl_3$), see Table 4; (+)-ESIMS *m/z* 749.3 $[M + H]^+$; (+)-HRESIMS *m/z* 771.2625 $[M + Na]^+$ (calcd for $C_{40}H_{44}O_{14}Na$, 771.2623).

Fortunilide I (**9**): white, amorphous powder; $[\alpha]^{24}_D$ +6.0 (*c* 0.4, MeOH); UV(MeOH) λ_{max} (log ε) 221 (4.42) nm; IR (KBr) ν_{max} 3433, 2930, 1751, 1441, 1220, 1153, 1081, 1012, 970 $cm^{-1;}$ ^{1}H NMR data (CD_3OD), see Table 3 and ^{13}C NMR (CD_3OD), see Table 4; (+)-ESIMS *m/z* 800.3 $[M - H_2O + H]^+$; (+)-HRESIMS m/z 805.2659 $[M + Na]^+$ (calcd for $C_{40}H_{46}O_{16}Na$, 805.2678).

Author Manuscript Author Manuscript Author Manuscript Author Manuscript

Fortunilide J (**10**): white, amorphous powder; $[\alpha]^{24}_{D}$ +107.9 (*c* 0.3, MeOH); UV(MeOH) λ_{max} (log ε) 208 (4.56) nm; IR (KBr) ν_{max} 3432, 2925, 1730, 1660, 1448, 1384, 1226, 1145, 959 $cm^{-1;}$ ^{1}H NMR data (CD_3OD), see Table 3 and ^{13}C NMR (CD_3OD), see Table 4; (−)-ESIMS *m/z* 635.6 $[M - H]^-$; (−)-HRESIMS *m/z* 635.2475 $[M - H]^-$ (calcd for $C_{35}H_{39}O_{11}$, 635.2498).

Fortunilide K (**11**): colorless gum; $[\alpha]^{24}_{D}$ −47.2 (*c* 1.0, MeOH); UV(MeOH) λ_{max} (log ε) 215 (4.37) nm; IR (KBr) ν_{max} 3455, 2926, 1761, 1656, 1444, 1377, 1252, 1133, 1092, 951 $cm^{-1;}$ ^{1}H NMR data ($CDCl_3$), see Table 3 and ^{13}C NMR ($CDCl_3$), see Table 4; (+)-ESIMS *m/z* 617.4 $[M + H]^+$; (−)-ESIMS *m/z* 615.7 $[M - H]^-$; (−)-HRESIMS *m/z* 615.2588 $[M - H]^-$ (calcd for $C_{36}H_{39}O_9$, 615.2600).

Fortunilide L (1**2**): colorless gum; $[\alpha]^{24}_{D}$ −26.9 (*c* 0.9, MeOH); UV(MeOH) λ_{max} (log ε) 215 (4.53) nm; IR (KBr) ν_{max} 3465, 2952, 1737, 1617, 1438, 1384, 1242, 1041, 968 $cm^{-1;}$ ^{1}H NMR data ($CDCl_3$), see Table 3 and ^{13}C NMR ($CDCl_3$), see Table 4; (+)-ESIMS *m/z* 747.5 $[M + H]^+$, *m/z* 769.3 $[M + Na]^+$; (−)-ESIMS *m/z* 745.8 $[M - H]^-$; (+)-HRESIMS *m/z* 769.2830 $[M + Na]^+$ (calcd for $C_{41}H_{46}O_{13}Na$, 769.2831).

Antiplasmodial Evaluation of Compounds 1–44

***P. falciparum in vitro* growth inhibition assay—**Dose-dependent growth inhibition against *P. falciparum* strain Dd2 (chloraquine-resistant) was measured in a 72 h growth assay in the presence of inhibitor as described previously.[30–31] Artemisinin was used as a positive control. Parasite growth was normalized to untreated controls in the presence of DMSO. Ring stage parasite cultures (100 μL per well, with 1% hematocrit and 1% parasitaemia) were grown for 72 h in the presence of increasing concentrations of the inhibitor in a 5.05% CO_2, 4.93% O_2 and 90.2% N_2 gas mixture at 37 °C. After 72 h in culture, parasite viability was determined by DNA quantitation using SYBR Green I as described previously. The half-maximum inhibitory concentration (IC_{50}) values were calculated with Kaleida Graph using nonlinear regression curve fitting, and the reported values represent averages of at least three independent experiments performed in triplicates with standard deviations.

Mammalian Cytotoxicity Evaluation of Selected Compounds with Antimalarial Activity

WI-38 cell line *in vitro* growth inhibition assay—Compounds were evaluated for their cytotoxicity against normal cell line WI-38 (normal embryonic lung tissue). Briefly, 10,000 cells per well were plated in a clear-bottom 96 well plate. Cells were allowed to adhere and then the media was replaced with 100 µL of media containing varying amounts of the test inhibitor and incubated for 24 h. After the incubation time was completed, 10 µL of resazurin sodium salt (Sigma) at 0.125 mg/mL was added to each well and incubated for 2 h. Cell viability was determined by measuring the fluorescence at 585 nm after excitation at 540 nm. The IC_{50} values were calculated as described above, and the reported values represent averages of at least two independent.

Supplementary Material

Refer to Web version on PubMed Central for supplementary material.

Author Manuscript Author Manuscript Author Manuscript Author Manuscript

Acknowledgments

This project was supported by the National Natural Science Foundation (No. 21532007, 81321092) and the Foundation (2012CB721105) from the Ministry of Science and Technology of the People's Republic of China. We thank Prof. S. Q. Tang of Guangxi Normal University for the identification of the plant of *C. fortunei*. The work of DGIK and MBC was supported by the National Center for Complementary and Integrative Health under award 1 R01 AT008088, and this support is gratefully acknowledged.

References

1. Greenwood BM, Bojang K, Whitty CJM, Targett GAT. Malaria. The Lancet. 2005; 365:1487–1498.
2. World Health Organization. World malarial report. http://www.who.int/malaria/publications/world-malaria-report-2015/report/en/
3. (a) Dondorp AM, Yeung S, White L, Nguon C, Day NP, Socheat D, von Seidlein L. Nat Rev Microbio. 2010; 8:272–280.(b) Dondorp AM, Nosten F, Yi P, Das D, Phyo AP, Tarning J, Lwin KM, Ariey F, Hanpithakpong W, Lee SJ. New Engl J Med. 2009; 361:455–467. [PubMed: 19641202] (c) White NJ. J Clin Invest. 2004; 113:1084–1092. [PubMed: 15085184] (d) Cowman AF, Morry MJ, Biggs BA, Cross G, Foote SJ. P Natl Acad Sci. 1988; 85:9109–9113.
4. Chen, YQ., Cheng, DZ., Wu, GF., Cheng, PS., Zhu, PZ. Zhongguo Zhiwu Zhi. Vol. 20. Science Press; Beijing: 1982. p. 80-96.
5. (a) Ni G, Zhang H, Liu HC, Yang SP, Geng MY, Yue JM. Tetrahedron. 2013; 69:564–569.(b) He XF, Yin S, Ji YC, Su ZS, Geng MY, Yue JM. J Nat Prod. 2009; 73:45–50.(c) Zhang S, Su ZS, Yang SP, Yue JM. J Asian Nat Prod Res. 2010; 12:522–528. [PubMed: 20552493] (d) Yuan T, Zhu RX, Yang SP, Zhang H, Zhang CR, Yue JM. Org Lett. 2012; 14:3198–3201. [PubMed: 22651226] (e) Yuan T, Zhang CR, Yang SP, Yin S, Wu WB, Dong L, Yue JM. J Nat Prod. 2008; 71:2021–2025. [PubMed: 19053511] (f) Zhang S, Yang SP, Yuan T, Lin BD, Wu Y, Yue JM. Tetrahedron Lett. 2010; 51:764–766.(g) Yang SP, Zhang CR, Chen HD, Liao SG, Yue JM. Chin J Chem. 2007; 25:1892–1895.(h) Yang SP, Yue JM. Tetrahedron Lett. 2006; 47:1129–1132.(i) Yang SP, Gao ZB, Wu Y, Hu GY, Yue JM. Tetrahedron. 2008; 64:2027–2034.(j) Yang SP, Gao ZB, Wang FD, Liao SG, Chen HD, Zhang CR, Hu GY, Yue JM. Org Lett. 2007; 9:903–906. [PubMed: 17263543]
6. (a) Schwikkard S, van Heerden FR. Nat Prod Rep. 2002; 19:675–692. [PubMed: 12521264] (b) Kaur K, Jain M, Kaur T, Jain R. Bioorg Med Chem. 2009; 17:3229–3256. [PubMed: 19299148]
7. (a) Ge H. Principal Prescription Emergency. AD 340; 2:111.(b) Klayman DL. Science. 1985; 228:1049–1055. [PubMed: 3887571]
8. Yunnan Zhongcaoyao. Yunnan People Press; Kunming: 1971. p. 80-96.
9. Wang QH, Kuang HX, Yang BY, Xia YG, Wang JS, Kong LY. J Nat Prod. 2010; 74:16–20. [PubMed: 21142110]
10. Kawabata J, Fukushi E, Mizutani J. Phytochemistry. 1995; 39:121–125.
11. Wang XC, Zhang YN, Wang LL, Ma SP, Liu JH, Hu LH. J Nat Prod. 2008; 71:674–677. [PubMed: 18303852]
12. Kim SY, Kashiwada Y, Kawazoe K, Murakami K, Sun HD, Li SL, Takaishi Y. Tetrahedron Lett. 2009; 50:6032–6035.
13. Kim SY, Kashiwada Y, Kawazoe K, Murakami K, Sun HD, Li SL, Takaishi Y. Chem Pharm Bull. 2011; 59:1281–1284. [PubMed: 21963639]
14. Li CJ, Zhang DM, Luo YM, Yu SS, Li Y, Lu Y. Phytochemistry. 2008; 69:2867–2874. [PubMed: 18929375]
15. (a) Tully L, Carson M, McMurry T. Tetrahedron lett. 1987; 28:5925–5928.(b) Yang SP, Gao ZB, Wang FD, Liao SG, Chen HD, Zhang CR, Hu GY, Yue JM. Org Lett. 2007; 9:903–906. [PubMed: 17263543]
16. Ran XH, Teng F, Chen CX, Wei G, Hao XJ, Liu HY. J Nat Prod. 2010; 73:972–975. [PubMed: 20392109]
17. (a) Demarco PV, Farkas E, Doddrell D, Mylari BL, Wenkert E. J Am Chem Soc. 1968; 90:5480–5486.(b) Yang SP, Gao ZB, Wu Y, Hu GY, Yue JM. Tetrahedron. 2008; 64:2027–2034.
18. He XF, Zhang S, Zhu RX, Yang SP, Yuan T, Yue JM. Tetrahedron. 2011; 67:3170–3174.

Author Manuscript Author Manuscript Author Manuscript Author Manuscript

19. Wang P, Luo J, Zhang YM, Kong LY. Tetrahedron. 2015; 71:5362–5370.
20. Kawabata J, Mizutani J. Phytochemistry. 1992; 31:1293–1296.
21. Fang PL, Cao YL, Yan H, Pan LL, Liu SC, Gong NB, Lü Y, Chen CX, Zhong HM, Guo Y. J Nat Prod. 2011; 74:1408–1413. [PubMed: 21650224]
22. Xu YJ, Tang CP, Ke CQ, Zhang JB, Weiss HC, Gesing ER, Ye Y. J Nat Prod. 2007; 70:1987–1990. [PubMed: 18044839]
23. Kawabata J, Mizutani J. Agri Biol Chem. 1989; 53:203–207.
24. Wang XC, Wu WQ, Ma SP, Liu JH, Hu LH. Chin J Nat Med. 2008; 6:404–407.
25. Kawabata J, Tahara S, Mizutani J. Agri Biol Chem. 1981; 45:1447–1453.
26. Yang SP, Yue JM. Tetrahedron Lett. 2006; 47:1129–1132.
27. Kim SY, Kashiwada Y, Kawazoe K, Murakami K, Sun HD, Li SL, Takaishi Y. Tetrahedron Lett. 2009; 50:6032–6035.
28. Kawabata J, Fukushi Y, Tahara S, Mizutani J. Phytochemistry. 1990; 29:2332–2334.
29. Kim SY, Kashiwada Y, Kawazoe K, Murakami K, Sun HD, Li SL, Takaishi Y. Phytochemistry Lett. 2009; 2:110–113.
30. Liu J, He XF, ang GH, Merino EF, Yang SP, Zhu RX, Gan LS, Zhang H, Cassera MB, Wang HY. J Org Chem. 2013; 79:599–607. [PubMed: 24344740]
31. Smilkstein M, Sriwilaijaroen N, Kelly JX, Wilairat P, Riscoe M. Antimicrob Agents Chemother. 2004; 48:1803–1806. [PubMed: 15105138]

Author Manuscript Author Manuscript Author Manuscript Author Manuscript

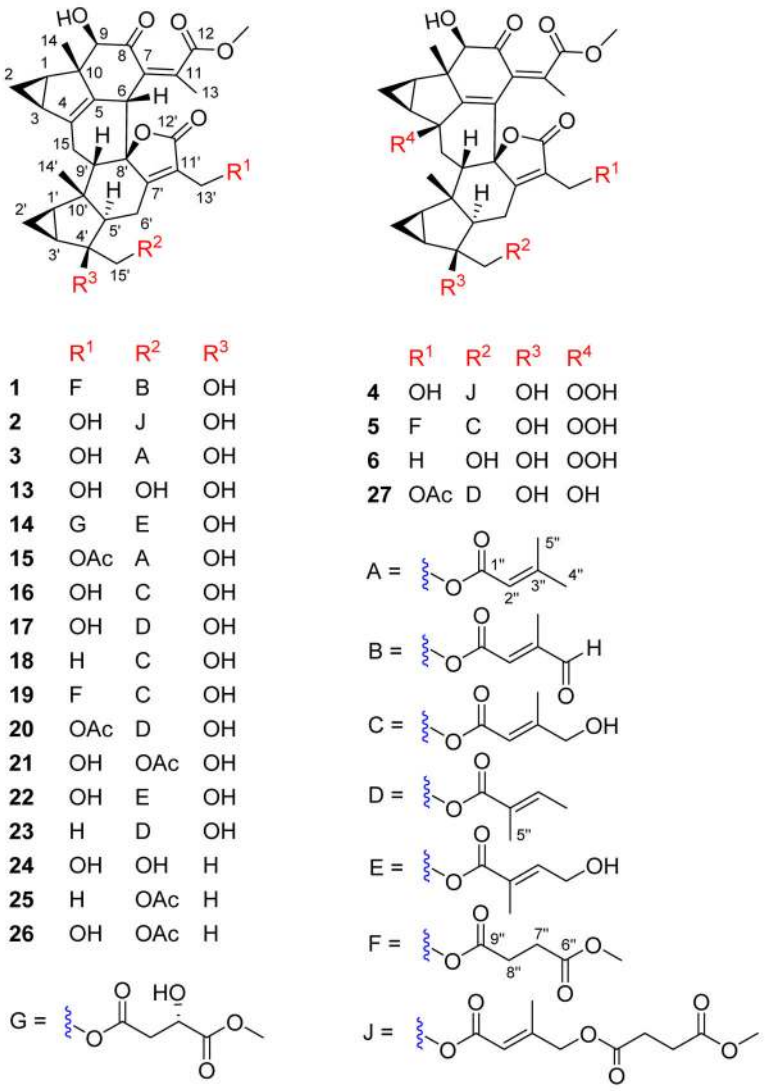

	R1	R2	R3
1	F	B	OH
2	OH	J	OH
3	OH	A	OH
13	OH	OH	OH
14	G	E	OH
15	OAc	A	OH
16	OH	C	OH
17	OH	D	OH
18	H	C	OH
19	F	C	OH
20	OAc	D	OH
21	OH	OAc	OH
22	OH	E	OH
23	H	D	OH
24	OH	OH	H
25	H	OAc	H
26	OH	OAc	H

	R1	R2	R3	R4
4	OH	J	OH	OOH
5	F	C	OH	OOH
6	H	OH	OH	OOH
27	OAc	D	OH	OH

Figure 1.
The tested compounds **1–6**, and **13–27**.

Author Manuscript Author Manuscript Author Manuscript Author Manuscript

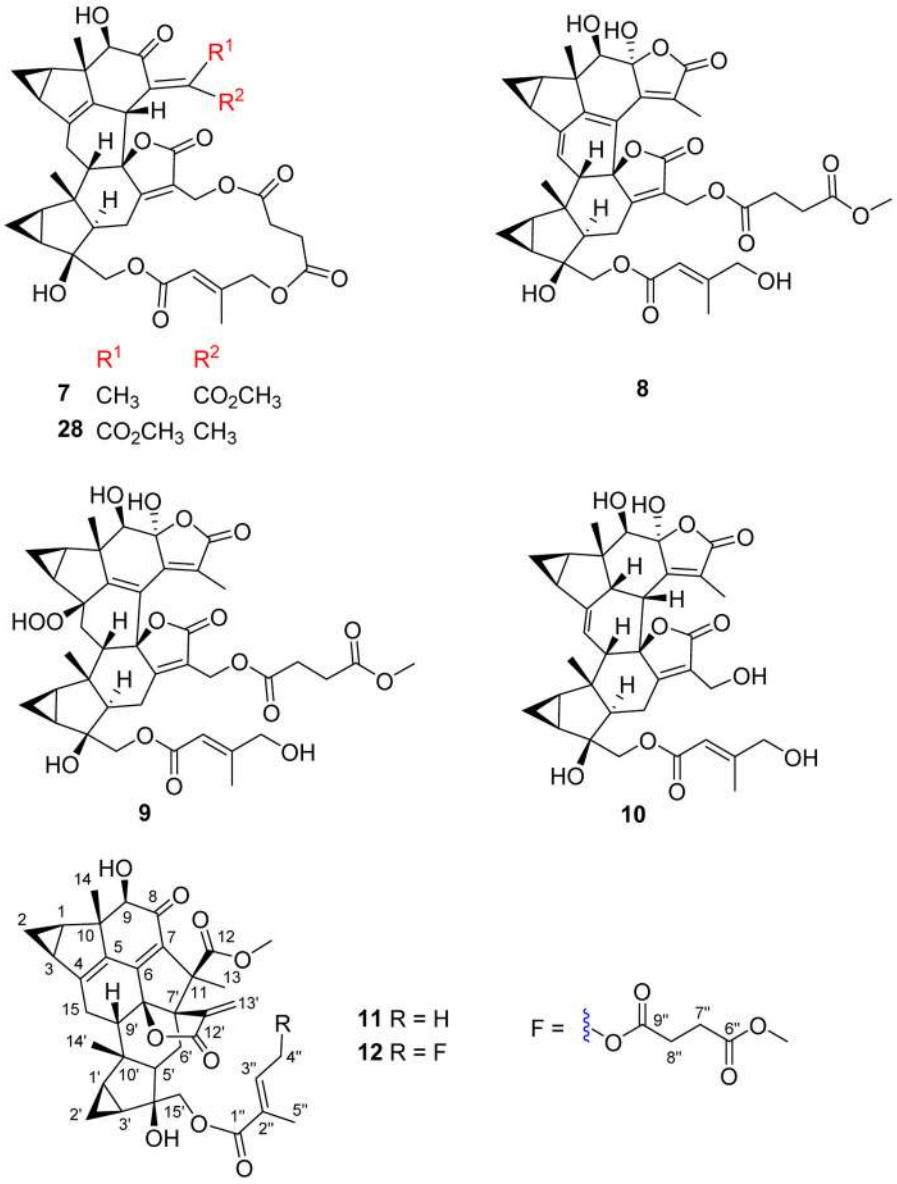

Figure 2.
The tested compounds **7–12**, and **28**.

Author Manuscript Author Manuscript Author Manuscript Author Manuscript

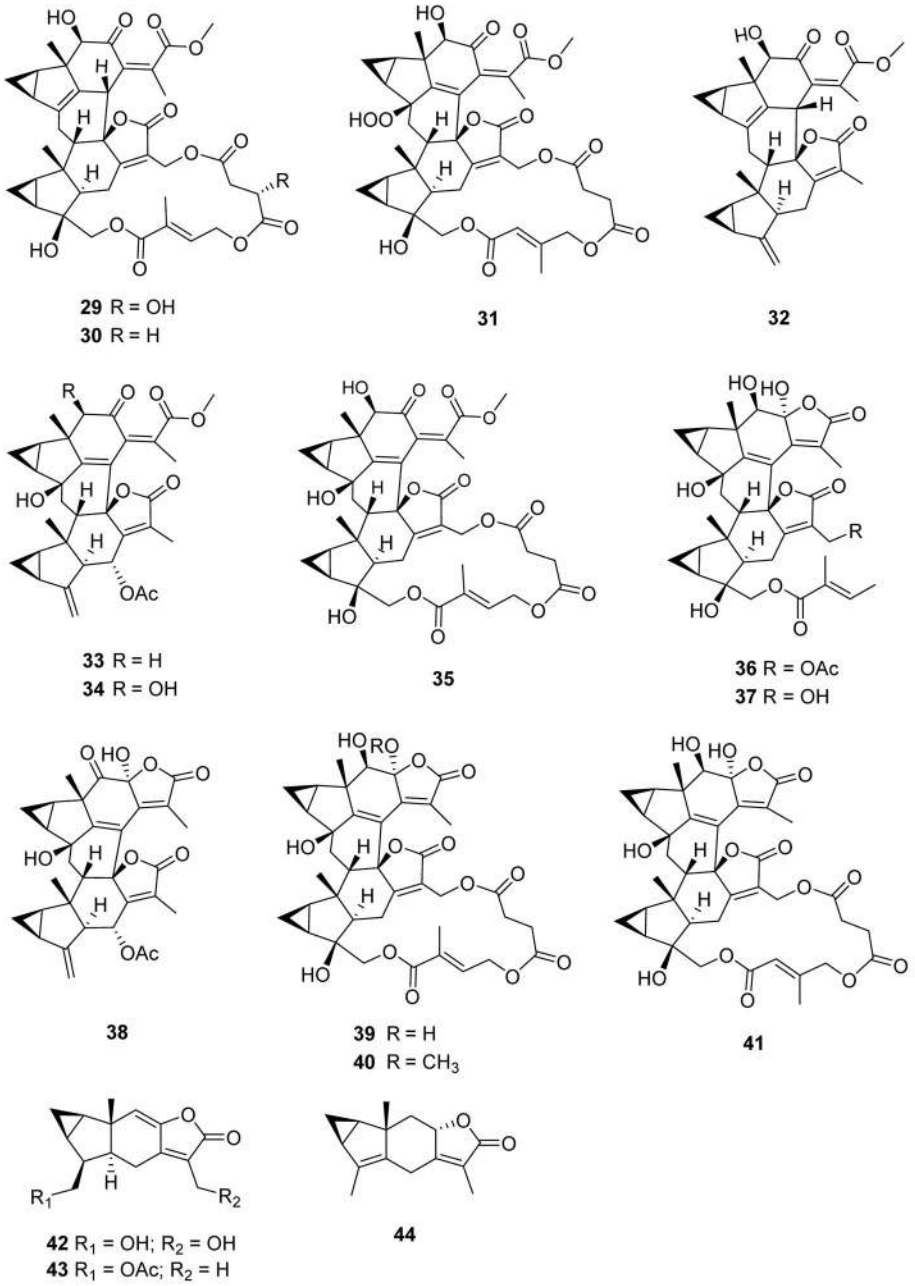

Figure 3.
The tested compounds **29–44**.

Author Manuscript Author Manuscript Author Manuscript Author Manuscript

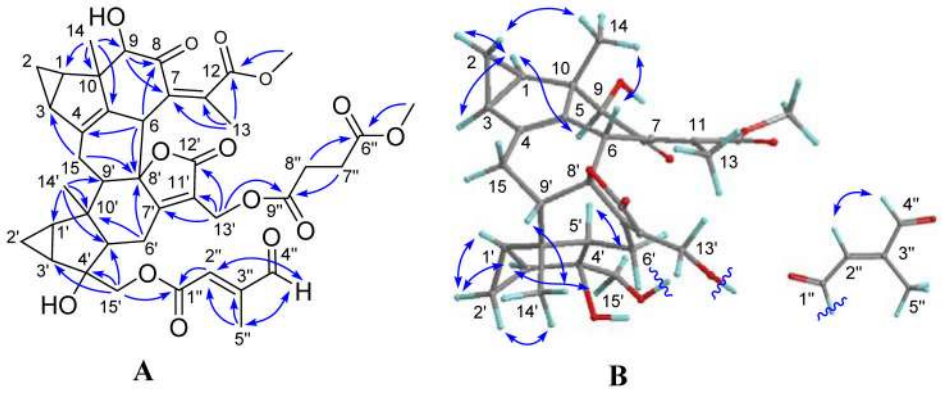

Figure 4.
(A) HMBC and (B) ROESY correlations of **1.**

Author Manuscript Author Manuscript Author Manuscript Author Manuscript

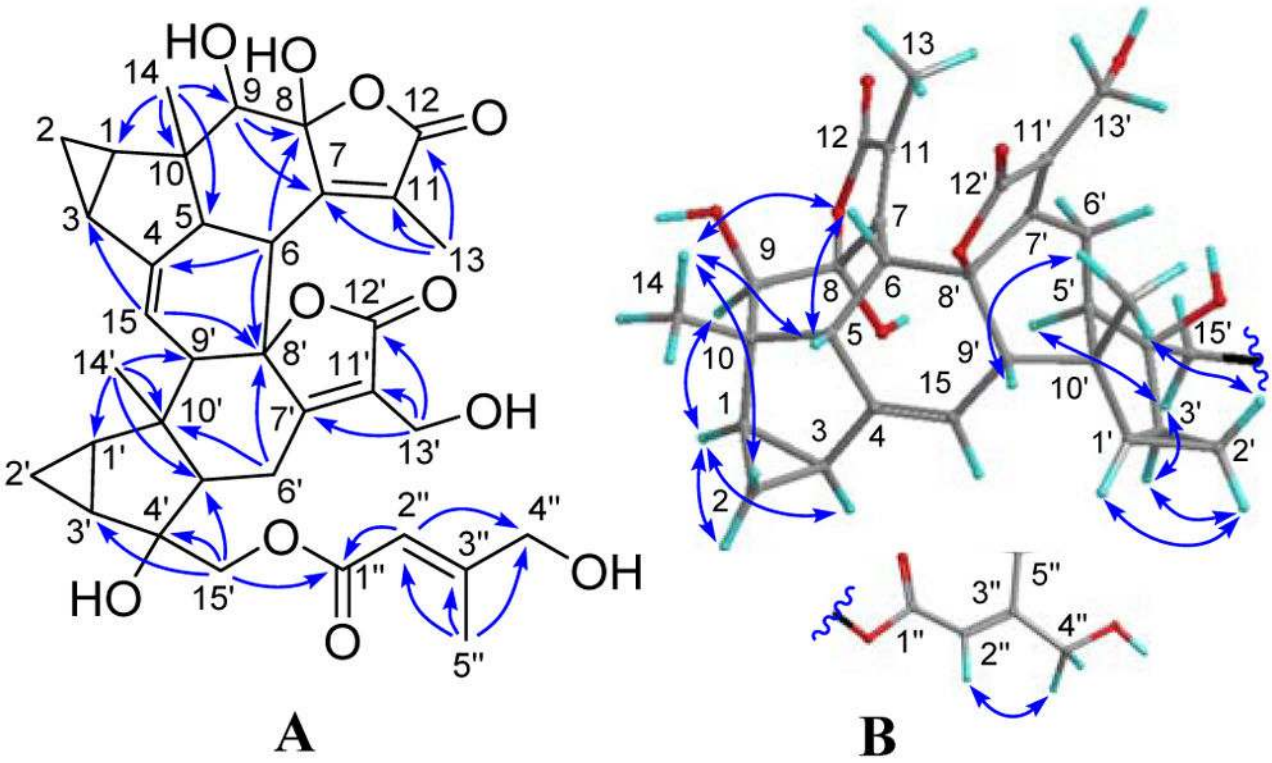

Figure 5.
(A) HMBC and (B) ROESY correlations of **10.**

Author Manuscript Author Manuscript Author Manuscript Author Manuscript

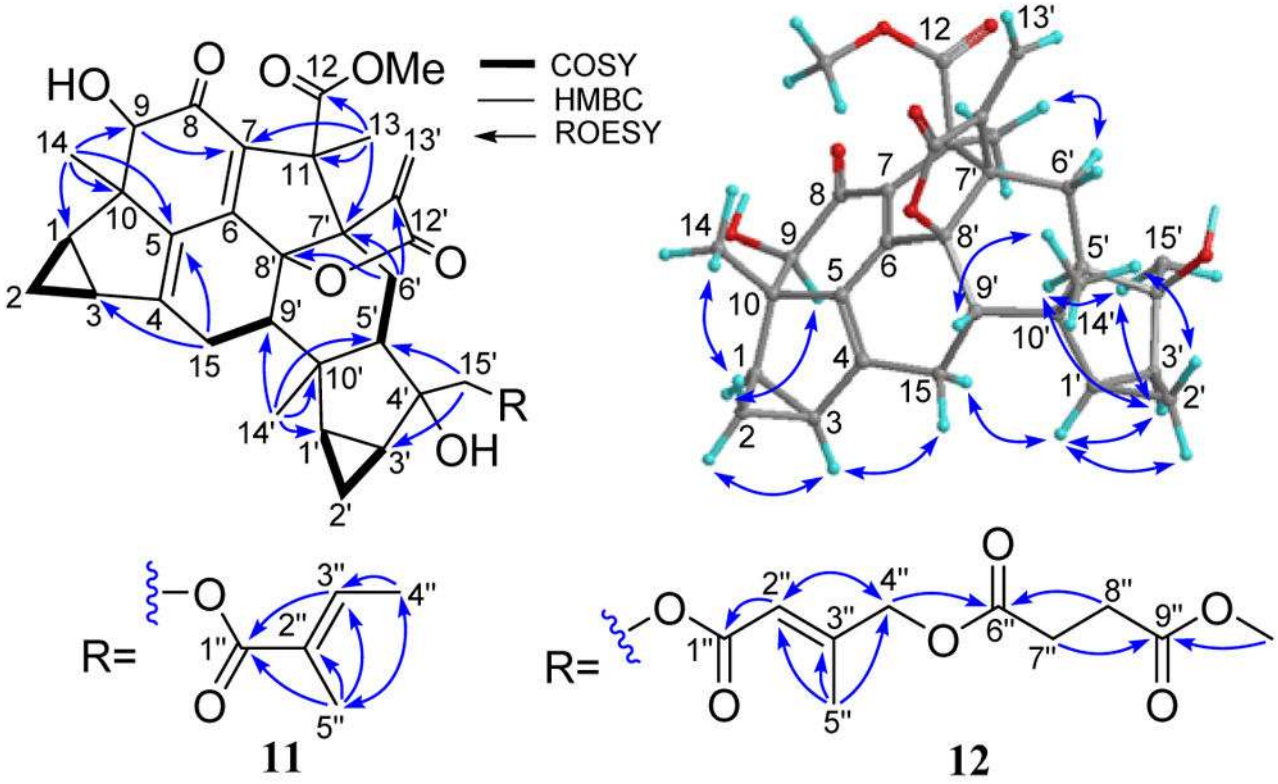

Figure 6.
Selected HMBC, COSY, and ROESY correlations of **11** and **12**.

Author Manuscript Author Manuscript Author Manuscript Author Manuscript

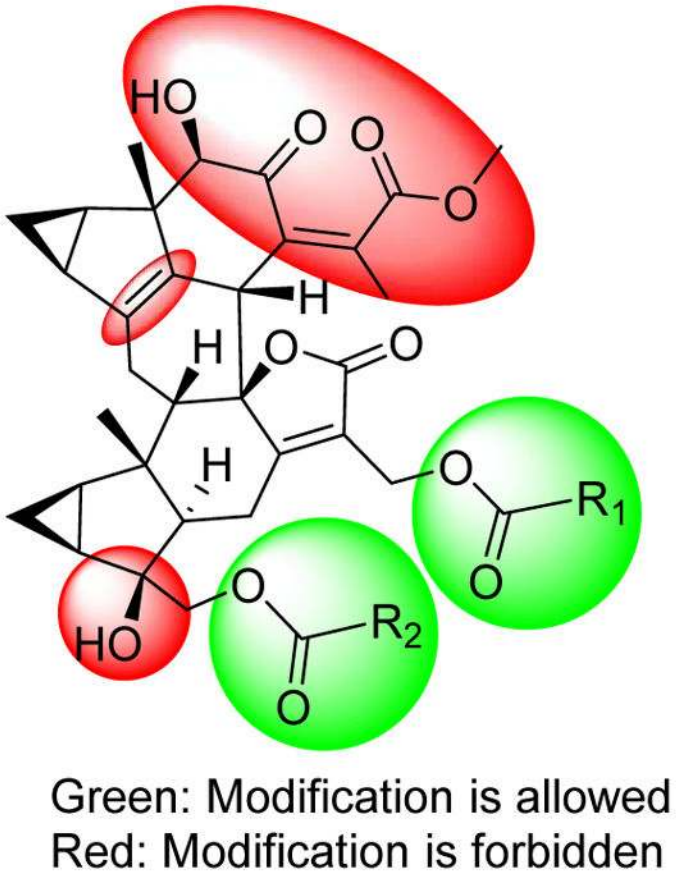

Figure 7.
Brief SAR of antiplasmodial compounds.

Author Manuscript Author Manuscript Author Manuscript Author Manuscript

Table 1

^{1}H NMR Data of Compounds 1–4 (500 MHz, $CDCl_3$)

No.	1	2	3	4
	(mult., *J* in Hz)	(mult., *J* in Hz)	(mult., *J* in Hz)	(mult., *J* in Hz)
1	2.05, ddd (8.3, 5.7, 4.2)	2.05, ddd (8.1, 5.7, 4.3)	2.08, ddd (8.3, 5.8, 4.2)	2.02, ddd (8.5, 6.2, 4.3)
2α	0.98, m	0.98, m	1.02, m	0.95, m
2β	0.27, m	0.29, m	0.33, m	1.26, m
3	1.83, m	1.82, m	1.87, m	1.57, m
6	3.93, d (3.7)	3.89, d (3.9)	3.93, d (3.9)	
9	3.95, s	3.92, s	3.97, s	3.78, s
13	1.87, s	1.90, s	1.94, s	1.78, s
14	1.00, s	0.98, s	1.02, s	1.01, s
15	2.75, m 2.60, m	2.78, m 2.55, ddd (16.4, 6.2, 3.9)	2.81, d (16.2) 2.58, ddd (16.2, 6.2, 3.9)	3.03, dd (14.2, 7.1) 1.61, m
1′	1.60, m	1.57, dt (8.4, 3.8)	1.60, dt (8.8, 5.7)	1.84, m
2′α	0.74, m	0.68, m	0.71, m	0.60, m
2′β	1.32, m	1.23, m	1.26, m	1.18, m
3′	1.45, m	1.49, ddd (9.0, 7.3, 3.8)	1.52, m	1.25, m
5′	1.81, m	1.82, m	1.87, dd (13.7, 6.1)	1.66, dd (13.2, 6.5)
6′α	2.52, dd (18.4, 5.8)	2.28, dd (18.5, 6.1)	2.28, dd (18.4, 6.1)	2.29, dd (17.6, 6.5)
6′β	2.77, m	2.72, m	2.72, dd (18.4, 13.7)	2.89, dd (17.6, 13.2)
9′	1.83, m	1.89, m	1.94, m	2.56, dd (10.2, 7.1)
13′	4.97, d (13.4) 4.82, d (13.4)	4.37, d (13.6) 4.30, d (13.6)	4.41, d (13.6) 4.34, d (13.6)	4.44, d (13.8) 4.37, d (13.8)
14′	0.88, s	0.85, s	0.88, s	0.98, s
15′	4.30, d (11.8) 3.83, d (11.8)	4.07, d (11.5) 3.81, d (11.5)	4.83, d (11.5) 4.10, d (11.5)	4.03, d (11.4) 3.97, d (11.4)
2″	6.65, q (1.5)	5.89, s	5.73, m	5.89, d (1.4)
4″	9.67, s	4.62, s	1.94, s	4.66, m
5″	2.19, d (1.5)	2.13, s	2.19, s	2.16, s
7″		2.67, m		2.67, m
8″		2.73, m		2.73, m
12-OMe	3.68, s	3.75, s	3.65, s	3.77, s
6″-OMe	3.66, s			
9″-OMe		3.67, s		3.69, s
4-OOH				8.64, s

Author Manuscript Author Manuscript Author Manuscript Author Manuscript

Table 2

^{1}H NMR Data of Compounds 5–8 at 500 MHz

No.	5[a]	6[b]	7[a]	8[a]
	(mult., *J* in Hz)	(mult., *J* in Hz)	(mult., *J* in Hz)	(mult., *J* in Hz)
1	1.98, m	1.98, ddd (8.3, 6.3, 4.3)	1.99, m	2.09, m
2α	0.95, m	0.94, ddd (8.3, 8.3, 5.7)	0.97, m	1.07, m
2β	1.24, m	1.00, ddd (5.7, 4.3, 4.0)	0.33, m	0.63, m
3	1.55, m	1.86, ddd (8.3, 6.3, 4.0)	1.80, m	2.21, m
6			4.65, br d	
9	3.85, s	3.94, s	3.77, s	3.85, s
13	1.78, s	1.69, s	2.05, s	1.75, s
14	1.00, s	1.05, s	1.05, s	0.81, s
15	3.06, dd (14.2, 7.1) 1.65, dd (14.2, 10.2)	3.20, dd (14.3, 7.2) 1.70, dd (14.3, 10.1)	2.73, m 2.50, m	6.16, d (4.6)
1′	1.87, m	1.50, ddd (8.9, 7.2, 4.0)	1.58, m	1.88, m
2′α	0.60, m	0.69, m	0.72, m	0.66, m
2′β	1.22, m	0.61, m	1.32, m	1.20, m
3′	1.55, m	1.32, m	1.37, m	1.71, m
4′		1.38, m		
5′	1.76, m	1.78 ddd (13.2, 11.0, 6.8)	1.76, m	2.26, dd (12.9, 6.1)
6′α	2.34, dd (17.7, 6.9)	2.34, dd (17.6, 6.8)	2.57, m	2.37, dd (18.5, 6.1)
6′β	2.82, dd (17.7, 13.2)	2.66, dd (17.6, 13.2)	2.83, m	2.82, dd (18.5, 12.9)
9′	2.58, dd (10.2, 7.1)	2.63, dd (10.1, 7.2)	1.76, m	2.65, m
13′	5.06, dd (13.7, 2.0) 4.78, d (13.7)	4.29, d (13.3) 4.24, d (13.3)	4.98, d (12.1) 4.50, d (12.1)	5.12, dd (13.2, 1.4) 4.81, d (13.2)
14′	0.96, s	0.85, s	0.77, s	0.98, s
15′	4.02, s	3.57, dd (10.5, 4.2) 3.35, dd (10.5, 6.2)	4.49, d (11.4) 3.65, d (11.4)	4.09, d (11.2) 3.87, d (11.2)
2″	5.90, dd (2.8, 1.5)		6.01, d (1.7)	5.98, m
4″	4.16, m		4.84, d (16.7) 4.59, d (16.7)	4.14, d (16.6) 4.09, d (16.6)
5″	2.19, d (1.5)		2.19, s	2.05, s
7″	2.64, m		2.58, m	2.50, m
8″	2.70, m		2.84, m	2.70, m
12-OMe	3.77, s	3.75, s	3.77, s	
6″-OMe	3.67, s			3.68, s
4-OOH	8.53, s			

[a]Data were measured in $CDCl_3$ and

[b]data were measured in CD_3OD.

Author Manuscript Author Manuscript Author Manuscript Author Manuscript

Table 3

^{1}H NMR Data of 9–12 at 500 MHz

No.	9[a]	10[a]	11[b]	12[b]
	(mult., *J* in Hz)	(mult., *J* in Hz)	δ_H (mult, *J* in Hz)	δ_H (mult, *J* in Hz)
1	1.91, ddd (8.7, 6.4, 4.7)	1.59, ddd (8.1, 5.8, 4.0)	2.18, dt (8.6, 4.9)	2.18, dt (8.6, 4.9)
2α	0.93, ddd (8.7, 5.7, 5.7)	0.58, m	1.17, m	1.18, m
2β	1.12, m	0.80, ddd (8.7, 8.1, 5.1)	0.62, m	0.62, m
3	1.82, ddd (8.5, 6.4, 3.8)	2.13, ddd (8.7, 5.8, 3.4)	1.96, ddd (2, 5.5, 3.1)	1.97, ddd (8.2, 5.4, 3.1)
5		2.20, m		
6		2.86, m		
9	3.78, s	3.97, s	3.94, s	3.99, s
13	1.56, s	1.84, s	1.35, s	1.38, s
14	0.77, s	1.07, s	1.16, s	1.16, s
15	3.22, dd (14.0, 6.9) 1.73, dd (14.0, 10.6)	5.82, s	2.30, dd (18.0, 7.1) 2.96, dd (18.0, 9.5)	2.29, dd (18.0, 7.2) 2.95, dd (18.0, 9.5)
1′	1.73, m	1.93, m	1.66, m	1.65, m
2′α	0.64, ddd (8.9, 5.3, 5.3)	0.63, m	0.64, m	0.64, m
2′β	1.22, m	1.20, m	1.20, m	1.20, m
3′	1.73, m	1.38, ddd (8.9, 7.3, 3.5)	1.66, m	1.66, m
5′	2.36, dd (12.7, 6.8)	2.49, dd (13.5, 5.6)	1.65, m	1.58, dd (14.6, 2.9)
6′α	2.46, dd (17.9, 6.8)	2.37, dd (18.7, 5.6)	2.45, d (13.0)	2.54, dd (14.6, 14.1)
6′β	2.91, dd (17.9, 12.7)	2.87, dd (18.7, 13.5)	1.69, m	1.73, dd (14.1, 2.9)
9′	2.71, dd (10.6, 6.8)	2.21, m	2.64, dd (9.5 7.1)	2.64, dd (9.5 7.2)
13′	4.87, d (13.3) 4.84, dd (13.3, 1.4)	4.37, d (13.2) 4.31, dd (13.2, 1.3)	5.52, brs 6.20, brs	5.51, brs 6.19, brs
14′	1.02, s	0.91, s	0.94, s	0.94, s
15′	4.04, d (11.0) 4.01, d (11.0)	4.41, d (11.2) 3.90, d (11.2)	4.23, d (11.1) 4.18, d (11.1)	4.30, d (11.1) 4.08, d (11.1)
2″	6.07, m	5.99, q (1.5)	6.86, m	5.91, q (1.5)
4″	4.10, m	4.08, m	1.81, brs	4.62, m
5″	2.12, d (1.3)	2.07, (br s)	1.82, brs	2.13, d (1.5)
7″	2.57, m			2.68, m
8″	2.67, m			2.75, m
12-OMe			3.44, s	3.43, s
6″-OMe	3.69, s			
9″-OMe				3.69, s

[a]Data were measured in CD_3OD and

[b]data were measured in $CDCl_3$.

Author Manuscript Author Manuscript Author Manuscript Author Manuscript

Table 4

^{13}C NMR Data of Compounds 1–12 at 125 MHz

No.	1[a]	2[a]	3[a]	4[a]	5[a]	6[b]	7[a]	8[a]	9[b]	10[b]	11[a]	12[a]
1	25.7	26.1	26.1	26.0	26.0	27.3	26.1	28.2	30.4	34.3	28.5	28.6
2	16.0	16.1	16.1	8.3	8.3	9.0	16.0	14.3	10.0	11.7	15.8	15.8
3	24.8	24.9	25.0	27.5	27.9	28.4	24.9	23.9	28.4	25.9	26.6	26.7
4	142.4	142.6	142.6	90.8	90.7	91.3	141.3	138.0	89.9	146.1	151.3	151.3
5	131.5	132.2	132.2	158.7	158.9	159.5	132.8	155.8	161.0	43.8	135.4	135.4
6	40.7	41.1	41.1	127.1	127.0	129.2	41.9	115.7	126.8	44.6	151.4	151.4
7	131.2	131.1	131.0	143.2	143.3	132.6	134.8	124.8	154.6	153.3	129.7	129.7
8	200.2	200.2	200.0	198.8	198.4	200.6	204.1	104.7	105.2	108.0	197.0	197.1
9	80.5	80.1	80.1	77.9	77.8	78.7	80.6	75.9	78.8	80.0	83.2	83.2
10	51.3	51.1	51.2	50.3	50.2	51.5	50.4	49.3	50.5	47.4	57.6	57.6
11	148.1	147.5	147.6	129.0	128.8	141.5	144.2	153.8	125.3	133.2	65.3	65.4
12	170.5	171.8	171.2	170.3	170.5	172.3	169.4	171.8	173.2	173.2	172.0	172.0
13	20.8	20.5	20.5	21.4	21.4	21.0	19.2	10.4	10.6	10.7	18.9	19.1
14	15.2	15.5	15.6	15.5	15.5	16.1	15.5	14.5	14.3	22.7	14.9	14.9
15	25.4	25.4	25.4	36.9	36.8	36.8	25.4	121.0	36.1	112.5	29.3	29.2
1′	25.6	25.7	25.7	27.9	27,5	27.4	26.2	25.6	28.2	26.6	26.6	26.6
2′	12.0	12.0	12.0	10.2	10.2	16.9	11.8	11.2	11.0	11.4	10.3	10.4
3′	28.0	28.4	28.6	29.3	29.0	24.1	27.2	29.2	30.4	29.8	29.8	29.7
4′	77.3	77.3	77.5	77.3	77.1	49.4	77.3	77.3	78.1	78.4	79.0	78.8
5′	61.0	59.9	59.8	54.6	54.0	54.5	61.8	55.8	53.1	57.1	55.7	56.5
6′	23.4	22.3	22.2	22.0	22.8	26.2	25.3	21.7	22.5	24.9	27.8	27.8
7′	171.9	168.5	168.5	166.3	170.3	170.0	174.4	171.6	173.9	173.2	59.1	59.1
8′	93.3	93.5	93.7	87.7	87.6	88.8	93.3	85.9	87.5	92.0	95.6	95.5
9′	55.9	55.1	55.1	52.7	52.8	52.4	55.0	55.5	52.1	54.0	52.2	52.1
10′	44.9	44.8	44.9	45.1	45.0	45.7	44.7	47.8	46.0	46.5	43.0	43.1
11′	123.6	127.5	127.4	128.6	125.3	129.5	123.2	123.6	124.7	128.4	145.9	146.1
12′	171.4	172.4	172.5	172.9	171.6	174.9	171.9	171.8	173.4	173.9	168.4	168.4
13′	55.8	54.8	54.9	55.1	55.8	54.5	55.2	55.3	56.6	54.6	123.1	129.7

Author Manuscript
Author Manuscript
Author Manuscript
Author Manuscript

No.	1[a]	2[a]	3[a]	4[a]	5[a]	6[b]	7[a]	8[a]	9[b]	10[b]	11[a]	12[a]
14′	26.6	26.4	26.4	24.4	24.3	23.1	26.2	25.3	24.5	25.8	24.0	24.0
15′	72.4	70.5	70.1	69.8	69.1	64.1	72.2	68.3	69.3	72.4	69.5	70.4
1″	165.5	166.1	166.8	166.0	166.3		166.2	167.0	168.4	168.3	167.9	166.0
2″	135.4	114.9	115.4	115.2	114.5		113.0	113.4	114.4	114.1	128.2	114.3
3″	151.2	153.4	158.8	153.9	160.9		153.9	159.1	159.9	160.1	138.7	154.2
4″	195.1	67.4	27.6	67.9	67.1		66.2	67.2	67.2	67.3	14.7	67.3
5″	11.0	15.9	20.6	16.1	15.8		15.9	16.0	16.0	15.8	12.3	16.0
6″	173.2	171.8		171.9	173.3		172.2	174.8	174.8			171.7
7″	28.7	28.8		28.9	28.6		29.5	28.5	173.9			28.9
8″	28.7	29.0		29.1	28.7		29.2	28.5	29.5			29.0
9″	172.1	173.0		173.0	172.1		172.9	171.9	29.5			172.9
12-OMe	52.8	52.9	52.9	53.0	53.1	53.1	53.0				52.2	52.1
6″-OMe	52.2				52.3			53.0	52.6			
9″-OMe		52.1		52.2								52.1

[a]Data were measured in $CDCl_3$ and

[b]data were measured in CD_3OD.

Author Manuscript Author Manuscript Author Manuscript Author Manuscript

Table 5

P. falciparum growth inhibition for compounds **1**–**44**

Comps	IC_{50} ± SD (nM)	Comps	IC_{50} ± SD (nM)
1	5.2 ± 0.6	**23**	320 ± 130
2	19 ± 8	**24**	11,400 ± 1,600
3	211 ± 56	**25**	1,800 ± 400
4	30 ± 8	**26**	580 ± 90
5	43 ± 3	**27**	IA
6	5,300 ± 2,000	**28**	11 ± 1
7	46 ± 3	**29**	13 ± 1
8	198 ± 22	**30**	27 ± 3
9	94 ± 30	**31**	474 ± 12
10	9,900 ± 2,700	**32**	1,500± 300
11	4,700 ± 500	**33**	IA
12	99 ± 18	**34**	IA
13	4,600 ± 200	**35**	IA
14	7.2 ± 1.3	**36**	IA
15	860 ± 89	**37**	IA
16	111 ± 12	**38**	IA
17	21 ± 9	**39**	IA
18	96 ± 37	**40**	IA
19	1.1 ± 0.2	**41**	7,100 ± 1,000
20	13 ± 3	**42**	IA
21	100 ± 10	**43**	IA
22	265 ± 5	**44**	IA

IA represents inactive (IC_{50} > 25 *m*M).

Artemisinin (IC_{50} = 4.0 ± 4.2 nM) was used as the positive control.

Author Manuscript Author Manuscript Author Manuscript Author Manuscript

Table 6

Mammalian cytotoxic activity (WI-38 cell line) of 15 most active natural compounds (IC_{50} ≤100 nM)

Compound	WI-38 IC_{50}(μM)	*P. falciparum* IC_{50}(μM)	SI
1	8.84	0.0052	1700
2	3.09	0.019	163
4	0.53	0.030	18
5	> 100	0.043	Not cytotoxic
7	1.24	0.046	27
12	15.5	0.099	157
14	4.04	0.0072	561
17	0.77	0.021	37
18	4.45	0.096	46
19	5.39	0.0011	4900
20	0.16	0.013	12
21	10.04	0.100	100
28	0.23	0.011	21
29	1.74	0.013	134
30	16.7	0.027	619
Adriamycin[a]	0.08	-	-

[a]adriamycin was used as the positive control